CFD Analysis of Liquid-Cooled Heatsink Using Nanofluids in Computer Processors

G. Topcu[1], U. Ercetin[2] and C. Timuralp[3,*]

1. Department of Mechanical Engineering, Kutahya Dumlupinar University, Kutahya, Turkey
gulnaztopcu@gmail.com
2. Department of Mechanical Engineering, Kutahya Dumlupinar University, Kutahya, Turkey
umran.ercetin@dpu.edu.tr
3. Department of Mechanical Engineering, Eskisehir Osmangazi University, Eskisehir, Turkey
cisil@ogu.edu.tr Phone:+90 222 2393750

In this study, a computer model of the Zalman ZM-WB3 Gold heat exchanger which is one of the liquid-cooled computer processors in the market has been generated and the model has been confirmed by the previous researchers' models and experimental data. Then, the fin thickness and heights of the same heat exchanger and the type of liquid fluid in which the heat exchanger operates have been changed. The CFD analyzes of the new models were performed by using Ansys Fluent 17.1 program. Following that, nano heat removal (cooling) performances were investigated with models using rectangular fin fluid heat exchangers with different fin heights of 5 mm, 5.5 mm and 5.7 mm, and different fin thicknesses of 1.2 mm, 1.4 mm, 1.6 mm, 1.8 mm and 2 mm, and different fluids as water, copper oxide-water (CuO-H_2O) nanofluids with volume ratios of 2.25% and 0.86%, and graphene oxide (GO-H_2O) nanofluid with the volume ratio of 0.01%. It was concluded that the best CPU cooler performance could be achieved by using CuO - H_2O as nanofluid with a volumetric ratio of 2.25% with a heat exchanger that has a 5.5 mm fin height and 2.0 mm fin thickness.

Keywords: CFD, CPU, Heatsink, Fin, Nanofluid, ANSYS/Fluent.

1. Introduction

With the rapid development of electronic devices in recent years, higher requirements for thermal cooling technology have been improved. While the performing speeds and capacities of electronic circuit elements and devices increased, the amount of heat per unit volume in electronic products increased significantly as well. The computer industry, especially computer processors, comes first among these sectors. The number of transistors placed in the processors increases with each new product, but the size problems and the removal of heat caused by the currents flowing through the transistors are still a big issue.

Most computer processors are designed as air-cooled, but air-cooled systems are insufficient for long-term and intensive processors. Nowadays, different solutions have been produced for the heating problems of the processors working in this way, and one of these solutions is the use of liquid-cooled processors [1]. While water has recently been used to remove heat from the limited surface area of computer processors, much larger heating and cooling systems use nanofluids with a higher thermal conductivity than water to generate better heat transfer [2-4].

Liquid fluids such as water, glycol and oil are generally used in heat transfer systems of many engineering applications such as ventilation, electronic cooling, and energy supply. Since the heat transfer coefficients of these fluids are not high, the heat transfer amount is also

limited. In order to increase the heat transfer performance of fluids, it was thought that the thermal conductivity of the fluids could be increased by adding small-sized conductive solid particles into the fluids, and studies in this direction were started and very nano-sized conductive solid particles were mixed into fluids to obtain nanofluids [5]. In the liquid phase, a fluid such as mineral oil, water and glycol or a mixture of more than one fluid is generally used in nanofluids. Metal powders such as copper (Cu), aluminum (Al), nickel (Ni) and metal oxides such as aluminum oxide (Al_2O_3) [6-13], copper oxide (CuO) [8-10,12-15], titanium oxide (TiO_2) [12,16], silicon oxide (SiO_2) [8,13] and carbon powders are used as nanoparticles. It has been stated in many studies in the literature that nanofluids show a better thermal performance than base fluid [17]. Mukesh Kumar and Arun Kumar [18] numerically investigated the heat transfer rate, surface temperature, Nusselt number, thermal resistance, power consumption and reliability of electronic chip in the six circular channel heat sink with water and the Al_2O_3/water nanofluids. They observed that the Al_2O_3/water nanofluids decreased the surface temperature, the power consumption and thermal resistance of electronic chip, increased the Nusselt number and the reliability of electronic chip.

In some studies, the effect of fin geometry and arrangement on heat transfer performance have been investigated. Vasilev et al. [19] performed a computational simulation of seventeen types of microchannel heat sink models in their another work. The channels equipped with circular pin fins having various diameters (0.25 and 0.5 mm), spacing (1.5, 3.0 and 6.0 mm) and height (0.1, 0.25, 0.4 and 0.5 mm) in order to compare their performance with the conventional microchannel heat sink. They observed that thermal resistance substantially depends on the height of the pins. The higher are the pins, the better is the heat flux. Khetib et al. [20] simulated the turbulent flow of a nanofluid in a channel. They used standard k-ε turbulence model and the SIMPLEC method to model the turbulent flow and to linearize the equations respectively. Their variables were fins type, fins arrangement, nanoparticle shape, and nanofluid velocity and their results show that increasing the velocity leads to decreasing in heatsink temperature and also using the brick-shaped nanoparticles and circular fins requires less pressure drop and give the best cooling performance. Saeed and Kim [21] presented a numerical investigation of minichannel heat sinks with different geometrical configurations by variation of fin spacing, fin thickness and fin height of the heat sink. They observed a reduction of 44.84% in base temperature for the heat sink with fin spacing and fin thickness of 0.2 mm and 0.4 mm respectively in comparison to un-finned geometry. Whelan et al. [22] designed and experimentally tested a liquid processor cooler to obtain a cooling capacity of 200 W for a surface area of 8.24 cm^2, proportional to the dimensions of the Intel Pentium 4 processor. They observed that when the base temperature of the water block was 53°C, the processor temperature was 65°C and they also calculated the thermal resistance of the system, 0.25 K/W and 0.18 K/W at 50 W and 200 W respectively.

Many researchers also have analyzed the effect of volume fraction of nanofluids. In the experimental study, Nazari et al. [23] tried to cooling the processor with nanofluids for four different speeds using aluminum oxide-water nanoplexers with volume fractions of 0.1%, 0.25% and 0.5%, CNT–water nanoplexers with volume fractions of 0.1% and 0.25%, and ethylene glycol with a volume percentage of 30% and 50%. According to their results, there was a 4% increase in convection heat transfer coefficient when ethylene glycol (30%) was used and a 6% increase when using 0.5% volume fraction of Alumina nanofluid. The best heat transfer increase (approximately 13%) obtained with CNT nanofluids of 0.25% volume fraction and 21 mL/s for the flow rate. Ghasemi et al. [24] experimentally and numerically studied the forced convection heat transfer and thermo-hydrodynamic properties of a cooler

using T_iO_2 nanofluid with different volume fractions and obtained a significant increase in the heat transfer coefficient when nanofluid was used. Saeed and Kim [25] experimentally and numerically investigated the heat transfer enhancement characteristics of a mini-channel heatsinks using nanofluid (Al_2O_3-H_2O) with two different volume concentrations and distilled water. Their results revealed that the convective heat transfer coefficient was enhanced significantly by using nanofluids in comparison with distilled water and predictions of two-phase mixture model were found in close agreement with an experimental model while single phase numerical model was found to have under predicted values of convective heat transfer coefficient. Mukesh Kumar and Arun Kumar [26] studied the heat sink's surface temperature, heat transfer rate, thermal resistance, power consumption and reliability by using CuO/water nanofluids at 0.25%, 0.5%, and 0.75% volume concentration as coolant and compared the nanofluids results with the results of water. Their numerical modelling, meshing and simulation were carried out by CATIAv5 and ANSYS Fluent v12 CFX software package. they observed that the heat transfer rates of semiconductor when used CuO/water nanofluid at 0.25%, 0.5%, and 0.75% volume concentrations are increased 25%, 43%, and 57% respectively. They found that the surface temperature of the semiconductor is lowered by 3%, 6%, and 8%, the thermal resistances decrease up to 6%, 10%, and 13%, and the Nusselt number increases by 25%, 43%, and 56% when compared to water. Yang et al. [27] studied the effects of adding Ag nano additives and Reynolds number on performance indicators in two microchannel heatsink. Their outcomes revealed that the augmentation of volume fraction of Ag nano additives and Reynolds number causes an increase in the convective heat transfer coefficient and a decrease in the CPU temperature. Wiriyasart et. al. [28] experimentally investigated the thermal performance of a compact heat sink thermoelectric cooling module with water, nanofluid and ferrofluid as the coolants. They tested the TiO_2 nanofluid and Fe_3O_4 ferrofluid at concentrations of 0.005% and 0.015%, respectively. Their results ferred out that the Fe_3O_4 ferrofluid showed a maximum heat transfer rate 11.17% and 12.57% higher, respectively, than that of the TiO_2 nanofluid and water. Zhao et al. [29] have experimentally studied the CPU cooler using TiO_2-water nanofluid in different volume fractions by slotting in three different ways with a diameter of 10 mm and a depth of 1 mm, 2 mm and 3 mm in the copper plate. They reported that the lowest processor temperature was achieved when used a nanofluid with a volume fraction of 0.3% and in a staggered arrangement with a groove depth of 2 mm and CPU surface temperatures was lowered by 3.3°C using nanofluids compared to deionized water. Bakhti and Si-Ameur [30] presented a numerical study on the mixed convection of nanofluids in heat sinks with perforated circular fins. They focused on to increase Reynolds number and decrease the volume fraction of nanoparticles to improve the heat transfer. Their results showed a significant improvement in heat transfer when they used nanofluids. Jahanbakhshi et al. [31] examined the effect of silver-water/ethylene glycol nanofluid volume fraction, Reynolds number and inlet and outlet arrangement on thermal performance and battery temperature changes in the microchannel and microtube. Their results demonstrated that the use of nanofluid in all cases reduces the battery surface temperature and keeps the temperature within a safe operating range. Al-Tae'y et al. [32] stated in their experimental work that the CPU temperature dropped from 42°C to 33°C at a flow rate of 0.0044 kg/h in a water-cooled copper cooler with rectangular cross-section channels with 1.6667 mm hydraulic diameter. They indicated that the heat transfer rate was 907.88 W/hr at full-load and it was 670.51 W/hr at a mass flow rate of 0.0177 kg/h for one hour. Qi et al. [33] analyzed the heat transfer enhancement of half-spherical bulges arrangements using TiO_2 nanofluids and they investigated the effect of groove depths and

aligned/staggered arrangements on thermal performances at CPU cooling. They stated that the best heat transfer was obtained with nanofluid with a volume fraction of 0.4%. Gorzin et al. [34] experimentally and numerically investigated the serpentine design to enhance thermal performance of the heat sink for liquid CPU cooling. They studied the effect of mass flow rate and the inlet temperature on the cooling performance of the maze serpentine. Their results indicated that by changing the minichannel design from straight to the proposed mazed shape geometry, baseplate temperature decreases 11.2% and Nusselt number increases 4.2 times in the maximum mass flow rate.

In this study, the CFD analysis of the models created by using Ansys Fluent 17.1 by changing the fin thickness and height of the heat exchanger used for cooling the computer processors and the fluid type was performed. Heat exchangers with different geometries were created with fin heights of 5.0 mm, 5.5 mm and 5.7 mm and fin thicknesses of 1.2 mm, 1.4 mm, 1.6 mm, 1.8 mm and 2 mm. The cooling performances of these geometries were investigated by using water, copper oxide-water (CuO-water) with a volume fraction of 2.25% and 0.86% and graphene oxide (GO-water) nanofluids with a volume fraction of 0.01% as a working fluid.

2. Problem Definition and Mathematical Model

In this study, the mini heat sink used in the experimental study by Al-Rashed et al. [2] is modeled and its dimensions are given in Figure 1. In their study, the outer diameter of the heat sink is 60 mm and its height is 13 mm, the fin's height and thickness are 5 mm and 1.6 mm., respectively and the distance between the fins is 1.45 mm. The fluid inlet and outlet diameters are 7 mm and the distance between their axes is 30 mm. The actual picture of the liquid cooler is shown in Figure 1-a, its technical drawing is shown in Figure 1-b, and the solid and fluid regions of the created model are shown in Figure 2. In this new study, after the proof of the model's accuracy, new models were designed by taking the fin heights of the CPU 5 mm, 5.5 mm and 5.7 mm and the fin thicknesses of 1.2 mm, 1.6 mm, 1.8 mm and 2 mm. Processor cooling performances were investigated by using water, copper oxide-water (CuO-H_2O) with volume fractions of 2.25% and 0.86% and graphene oxide (GO-H_2O) with volume fractions of 0.01% as fluid. 115 W was applied to the CPU surface area. It was assumed that the fluid enters the CPU cooler at a constant flow rate of 0.05 kg/s and 303 K.

In this study, different volumetric fractions of copper oxide-water and graphene oxide-water nanofluids were used and thermophysical properties of fluids are given in Table 1 [2,35].

The Reynolds number for the fluid at constant flow is calculated with Equations (1) and (2) [36] and calculated velocity values and Re numbers are given in Table 2. A turbulence model is applied for the solution.

$$\dot{m} = \rho V A \tag{0}$$

$$Re = \frac{\rho V_{ave} D}{\mu} \tag{2}$$

The governing equations are stated as follows;

For the continuity

$$\frac{\partial u}{\partial x}+\frac{\partial v}{\partial y}+\frac{\partial w}{\partial z}=0 \tag{3}$$

x-momentum

$$\rho\left(u\frac{\partial u}{\partial x}+v\frac{\partial u}{\partial y}+w\frac{\partial u}{\partial z}\right)=-\frac{\partial P}{\partial x}+\mu\left(u\frac{\partial^2 u}{\partial x^2}+v\frac{\partial^2 u}{\partial y^2}+w\frac{\partial^2 u}{\partial z^2}\right)+\rho g_x \tag{4}$$

y-momentum

$$\rho\left(u\frac{\partial v}{\partial x}+v\frac{\partial v}{\partial y}+w\frac{\partial v}{\partial z}\right)=-\frac{\partial P}{\partial y}+\mu\left(u\frac{\partial^2 v}{\partial x^2}+v\frac{\partial^2 v}{\partial y^2}+w\frac{\partial^2 v}{\partial z^2}\right)+\rho g_y \tag{5}$$

z-momentum

$$\rho\left(u\frac{\partial w}{\partial x}+v\frac{\partial w}{\partial y}+w\frac{\partial w}{\partial z}\right)=-\frac{\partial P}{\partial z}+\mu\left(u\frac{\partial^2 w}{\partial x^2}+v\frac{\partial^2 w}{\partial y^2}+w\frac{\partial^2 w}{\partial z^2}\right)+\rho g_z \tag{6}$$

Energy

$$u\frac{\partial T}{\partial x}+v\frac{\partial T}{\partial y}+w\frac{\partial T}{\partial z}=-\left(\frac{k}{\rho c_p}\right)+\left(\frac{\partial^2 T}{\partial x^2}+\frac{\partial^2 T}{\partial y^2}+\frac{\partial^2 T}{\partial z^2}\right) \tag{7}$$

In this study, the "Realizable k-epsilon" model was applied and the calculations of k and ε in this model are given in Equations (8) and (9).

$$\frac{\partial}{\partial t}(\rho k)+\frac{\partial}{\partial x_j}(\rho k u_j)=\frac{\partial}{\partial x_j}\left[\left(\mu+\frac{\mu_t}{\sigma_k}\right)\frac{\partial k}{\partial x_j}\right]+G_k+G_b-\rho\varepsilon-Y_M+S_k \tag{8}$$

$$\frac{\partial}{\partial t}(\rho\varepsilon)+\frac{\partial}{\partial x_j}(\rho\varepsilon u_j)=\frac{\partial}{\partial x_j}\left[\left(\mu+\frac{\mu_t}{\sigma_\varepsilon}\right)\frac{\partial \varepsilon}{\partial x_j}\right]+\rho C_1 S\varepsilon-\rho C_2\frac{\varepsilon^2}{k+\sqrt{v\varepsilon}}+C_{1\varepsilon}\frac{\varepsilon}{k}C_{3\varepsilon}G_b+S_\varepsilon \tag{9}$$

In these Equations, G_k is the generation of turbulence kinetic energy due to the mean velocity gradients, G_b represents the generation of turbulence kinetic energy due to buoyancy, Y_M is the contribution of the fluctuating dilatation incompressible turbulence to the overall dissipation rate, C_1 and $C_{1\varepsilon}$ are constants, σ_k and σ_ε are the turbulent Prandtl numbers for k and ε, S_k and S_ε are user-defined source terms.

$$C_1=max\left[0.43\frac{\eta}{\eta+5}\right] \tag{10}$$

$$\eta = S\frac{k}{\varepsilon} \tag{11}$$

$$S = \sqrt{2S_{ij}S_{ij}} \tag{12}$$

$$\mu_t = \rho C_\mu \frac{k^2}{\varepsilon} \tag{13}$$

Here, μ_t is the turbulence viscosity and C_μ is the constant.

$$G_k = \mu_t S^2 \tag{14}$$

$$G_b = -g_i \frac{\mu_t}{\rho Pr_t}\frac{\partial \rho}{\partial x_i} \tag{15}$$

$$C_{3\varepsilon} = tanh\left|\frac{v}{u}\right| \tag{16}$$

3. Numerical Solution and Grid Structure

The numerical simulations were carried out using finite volume method-based CFD commercial program AnsysFluent® 17.1. The geometry was drawn with Ansys Design Modeler, the mesh structure was made in ANSYS ICEM CFD and the three-dimensional steady-state continuity, Navier Stokes and energy equations were solved in AnsysFluent [37]. For momentum and energy calculations second-order upwind discretization scheme and for the solution algorithm SIMPLE were used. The convergence criteria were set as 10^{-3} for velocity, k and ε values, and 10^{-6} for energy. The mesh structure was generated by the cutcell method and 1162441 elements, 980239 in the solid domain and 182202 in the fluid domain, were used in the solution. The maximum skewness value was 0.92034 and the minimum orthogonal value was 0.29079 which are among the values stated as decent.

Also, solutions were made with tetrahedron elements in 4 different mesh numbers between 595253 and 4648881, the same results were obtained and it was seen that the solution was independent of the mesh number. Moreover, the solutions are repeated with cutcell mesh and it has been proven that the solution is independent of the mesh shape. Solutions show cutcell mesh solutions due to solution advantages of hexahedral mesh elements.

4. Results and Discussion

In the solutions, temperature and velocity distributions in the heat exchanger were examined using different fluids at different fin heights and thicknesses. Fig 3 and Fig 4 demonstrate the variation of the CPU temperature with different fin heights and fin thicknesses when using different volumetric fractions of nanofluid. For the figures, “a” indicates the fin height and “b” indicates the fin thickness. For all fin heights and thicknesses,

the highest processor temperature is obtained when water is used as the fluid. This is followed by 0.01% GO-water, 0.86% CuO-water and the lowest temperature is achieved in the case of 2.25% Cu0-water. When the investigated geometries were compared, the highest temperature was obtained for a=5.5 and b=1.2 case and the lowest temperature for a=5.5 and b=2 case. In the use of nanofluids, increasing the volumetric fraction also caused a decrease in temperature. When using GO-water as a working fluid, the temperature was observed somewhat higher than CuO-water.

Fig 5 shows the contours of temperature distribution for the fin height of 5.5 mm and the fin thicknesses of 1.2 mm (left column) and 2 mm (right column) in the use of different working fluids. As stated before, in both cases, the highest processor temperature was obtained with the use of water, while the lowest temperature was obtained using CuO-H_2O with a volume fraction 2.25%. For the left column in Fig 5a, the maximum temperature is 311.12 K while the temperature is 310.67 K in Fig 5d. For the right column, these temperatures are slightly reduced and are measured 310.1 K and 309.74 K, respectively. It has been found that nanofluids show better cooling performance. Besides, the nanofluid obtained by using copper oxide nanoparticles gave a better result than the nanofluid obtained with the graphene oxide nanoparticles. A decrease in temperature inside the processor has been observed with the increase in fin thickness.

The graphs of the calculated thermal resistances and heat convection coefficients in the case of using different fluids in the heat sink with a fin length of 5.5 mm and a fin thickness of 2 mm are shown in Figures 6 and 7. The thermal resistance and heat convection coefficient values calculated for 115 W heat transfer from the CPU surface to the fluid in the heat exchanger are partially in agreement with the results of the study by Al-Rashed et al. [2]. While Al-Rashed et al. estimated the thermal resistance of water between approximately 0.08 and 0.098 K/W in the case of water flowing in the heat sink, these values were estimated between 0.054 and 0.088 K/W ($^oC/W$) in our modelling. Other thermal resistances we obtained from our model are between 0.052 and 0.084 for 0.86% CuO-Water nanofluid and between 0.051 and 0.082 for 2.25% CuO-Water nanofluid. The lowest thermal resistances obtained by Al-Rashed et al. in the range of 0.02-0.08 kg/s flow rate are higher than the thermal resistance values we estimated. This is because Al-Rashed et al. used a laminar model in their modeling, whereas we used a turbulent model in our study. The reason for choosing the turbulent model is that the fluid entering the heat sink does not flow at the same rate in all channels, and in fact, there is turbulent flow in many channels in the heat sink.

Heat convection coefficients in our model, in the range of 0.01-0.05 kg/s mass flow rate, are 1986-3229 W/m^2K for water, 2103-3371 W/m^2K for 0.01% GO-Water nanofluid, 2090-3398 W/m^2K for 0.86% CuO-Water nanofluid and 2133-3445 W/m^2K for 2.25% CuO-Water nanofluid.

In Figure 8, the graph of Nu values and pressure drop values is given in the case of only water flowing at different flow rates in the heat exchanger. As can be seen from the graphics, Nusselt values vary between 4.99-8.16, while the pressure loss in the heat exchanger varies between 80-1444 Pa. These values are very similar to the values in the literature.

5. Conclusion

In this study, Zalman ZM-WB3 Gold liquid fluid CPU heat exchanger, which was experimentally and numerically modeled by Al-Rashed et al. [2], was modeled using the ANSYS Fluent program. With the created model, the results of the experimental and

numerical models of Al-Rashed et al. were obtained exactly, then the effects of the fin thickness and height on the heat transfer were investigated numerically by using water and different nanofluids by changing the distance between the fins of the heat exchanger, the thickness and height of the fins. For the modeling, the independence of the grid has been tested and it has been shown that the results obtained are mesh independent of the grid.

In the study, the cooling performance of the Zalman ZM-WB3 Gold heat exchanger, which is still used as a liquid-fluid CPU cooler in the market, has been tried to be increased. For this purpose, this heat exchanger was modeled numerically by increasing the fin thicknesses from 1.2 mm to 2 mm in 0.2 mm intervals and changing the fin heights according to these values. These models were first solved with water and then using nanofluids.

According to the results obtained, it was determined that the cooling performance increased as the fin thickness increased, and the cooling performance increased when the fin thickness was kept constant and the fin heights were changed. In numerical models, when nanofluid is used instead of water, the cooling performance has increased but the amount of increase was small. Due to the small size of the heat exchanger, the use of nanofluids was not very effective in improving the cooling performance.

Comparing the efficiency of nanofluids, it was seen that copper-water nanofluid gave better results than graphene oxide-water nanofluid. In addition, in CuO-water nanofluids, the nanofluid with a volume fraction of 2.25% gave a better cooling performance than a nanofluid with a volume fraction of 0.86%. Increasing the volume ratio of nanofluids also increased the cooling performance. When the efficiency of nanofluids is compared with water for a mass flow rate of 0.05 kg/s; 2.25% CuO-water nanofluid 6.69%, 0.86% CuO-water nanofluid 5.25% and 0.01% GO-water nanofluid improved heat transfer by 4.42%.

When the thermal resistance of 2.25% CuO-water nanofluid, which has the lowest thermal resistance for a mass flow rate of 0.05 kg/s, is compared with the thermal resistances of other fluids, the thermal resistance of water is 6.69%, the thermal resistance of 0.01% GO-water nanofluid is 2.18% and the thermal resistance of 0.86% CuO-water nanofluid is 1.37% greater than that of 2.25% CuO-water nanofluid.

Considering all the models made, the best CPU cooler performance was obtained when using CuO-water nanofluid with 5.5 mm fin height and 2.0 mm fin thickness and 2.25% volumetric ratio. The worst cooling performance of the heat sink was obtained when 5.5 mm fin height and 1.2 mm fin thickness were used and water was used as the working fluid.

Nomenclature

CFD	Computational Fluid Dynamics
CNT	Carbon nanotubes
CPU	Central Process Unit
CuO	Copper oxide
GO	Graphen oxide
K	Kelvin
W	Watt
hr	Hour
$\dot{m}$	Mass flow rate (kg/s)
ρ	Density (kg/m^3)
V	Velocity (m/s)
Re	Reynolds number
D	Diameter (m)
c_p	Specific heat (J/kgK)

μ Dynamic viscosity (kg/ms)
k Thermal conductivity (W/mK) / Turbulence kinetic energy
G_k Generation of turbulence kinetic energy due to the mean velocity gradients
G_b Generation of turbulence kinetic energy due to buoyancy
Y_M Contribution of the fluctuating dilatation incompressible turbulence to the overall dissipation rate
C_1 Constant
$C_{1\varepsilon}$ Constant
σ_k Turbulent Prandtl numbers for k
σ_ε Turbulent Prandtl numbers for ε
ε Disspation rate of turbulence kinetic energy
S_k User-defined source terms
S_ε User-defined source terms
μ_t Turbulence viscosity
C_μ Constant

References

1. Ma, K. and Liu, J. "Liquid metal cooling in thermal management of computer chips" , *Frontiers of Energy and Power Engineering in China*, **1**, pp. 384–402 (2007).
2. Al-Rashed, M.H., Dzido, G., Korpyś, M., et.al., "Investigation on the CPU nanofluid cooling", *Microelectronics Reliability*, **63**, pp. 159-165 (2016).
3. Colangelo, G., Favale, E., Milanese M., et.al., "Cooling of electronic devices: Nanofluids contribution", *Applied Thermal Engineering*, **127**, pp. 421-435 (2017).
4. Salman, B.H., Mohammed, H.A., Munisamy, K.M., et.al., "Characteristics of heat transfer and fluid flow in microtube and microchenneel using conventional fluids and nanofluids: A review", *Renewable and Sustainable Energy Reviews*, **28**, pp. 848-880 (2013).
5. Wang, X. and Mujumdar, A.S., "A Review on Nanofluids-Part II: Experiments and Applications", *Brazilian Journal of Chemical Engineering*, **25(4)**, pp. 631-648 (2008).
6. Somesekhar, K., Malleswara Rao, K.N.D., Sankararao, V., et.al., "A CFD Investigation of Heat Transfer Enhancement of Shell and Tube Heat Exchanger Using Al_2O_3-Water Nanofluid", *Materials Today: Proceedings*, **5(1)**, pp. 1057-1062 (2018).
7. Zeiny, A., Al-Bahhdadi, M.A.R., Arear, W.F., et.al., "Al_2O_3–H_2O nanofluids for cooling PEM fuel cells: A critical assessment", *International Journal of Hydrogen Energy*, **47(91)**, pp. 38823-38836 (2022).
8. Al-Baghdadi, M., Noor, Z., Zeiny, A., et.al., "CFD analysis of a nanofluid-based microchannel heat sink", *Thermal Science and Engineering Progress*, **20**, 100685 (2020).
9. Narendar, G. and Tejo Satya Charisma, K., "CFD study on the effect of nanofluids in natural circulation loop", *Materials Today: Proceedings*, **49(5)**, pp. 2116-2123 (2022).
10. Ferr˜ao Teixeira Alves, L.O., Henríquez, J.R., da Costa, J. A., et.al., "Comparative performance analysis of internal combustion engine water jacket coolant using a mix of Al_2O_3 and CuO-based nanofluid and ethylene glycol", *Energy*, **250**, 123832 (2022).
11. Kim, S., Song, H., Yu, K., et.al., "Comparison of CFD simulations to experiment for heat transfer characteristics with aqueous Al_2O_3 nanofluid in heat exchanger tube", *International Communications in Heat and Mass Transfer*,**95**, pp.123-131 (2018).

12. Özenbiner, Ö. and Yurddaş, A., "Numerical analysis of heat transfer of a nanofluid counter-flow heat exchanger", *International Communications in Heat and Mass Transfer*, **137**, 106306 (2022).
13. Hasan, H.A., Hatem, A.A., Abd, L.A., et.al., "Numerical investigation of nanofluids comprising different metal oxide nanoparticles for cooling concentration photovoltaic thermal CPVT", *Cleaner Engineering and Technology*, **10**, 100543 (2022).
14. Cruz, P.A.D., Yamat, E.E., Nuqui, J.P.E., et.al., "Computational Fluid Dynamics (CFD) analysis of the heat transfer and fluid flow of copper (II) oxide-water nanofluid in a shell and tube heat exchanger", *Digital Chemical Engineering*, **3**, 100014 (2022).
15. El-Khouly, M. M., El Bouz, M. A. and Sultan, G. I., "Experimental and computational study of using nanofluid for thermal management of electronic chips", *Journal of Energy Storage*, **39**, 102630 (2021).
16. Moraveji, M.K., Ardehali, R.M., Ijam, A., "CFD investigation of nanofluid effects (cooling performance and pressure drop) in mini-channel heat sink", *International Communications in Heat and Mass Transfer*, **40**, pp. 58-66 (2013).
17. Raja, M., Vijayan, R., Dineshkumar, P., et.al., "Review on nanofluids characterization, heat transfer characteristics and applications", *Renewable and Sustainable Energy Reviews*, **64**, pp. 163-173 (2016).
18. Mukesh Kumar, P.C. and Arun Kumar, C.M., "Numerical study on heat transfer performance using Al2O3/water nanofluids in six circular channel heat sink for electronic chip", *Materials Today: Proceedings*, **21(1)**, pp.194-201 (2020).
19. Vasilev, M.P., Abiev, R.Sh and Kumar, R., "Effect of circular pin-fins geometry and their arrangement on heat transfer performance for laminar flow in microchannel heat sink", *International Journal of Thermal Sciences*, **170**, 107177 (2021).
20. Khetib, Y., Sedraoui, K., Melaibari, A.A., et.al., "Heat transfer and pressure drop in turbulent nanofluid flow in a pin-fin heat sink: Fin and nanoparticles shape effects", *Case Studies in Thermal Engineering*, **28**, 101378 (2021).
21. Saeed, M. and Kim, M.H., "Numerical study on thermal hydraulic performance of water cooled mini-channel heat sinks", *International Journal of Refrigeration*, **69**, pp. 147-164 (2016).
22. Whelan, B.P., Kempers, R. and Robinson, A.J., "A liquid-based system for CPU cooling implementing a jet array impingement waterblock and a tube array remote heat exchanger", *Applied Thermal Engineering*, **39**, pp. 86-94 (2012).
23. Nazari, M., Karami, M., Ashouri, M., "Comparing the thermal performance of water, Ethylene Glycol, Alumina and CNT nanofluids in CPU cooling: Experimental study", *Experimental Thermal and Fluid Science*, **57**, pp. 371-377 (2014).
24. Ghasemi, S. E., Ranjbar, A.A., Hosseini, M.J., "Forced convective heat transfer of nanofluid as a coolant flowing through a heat sink: Experimental and numerical study", *Journal of Molecular Liquids*, **248**, pp. 264-270 (2017).
25. Saeed, M. and Kim, M.H., "Heat transfer enhancement using nanofluids (Al_2O_3-H_2O) in mini-channel heatsinks", *International Journal of Heat and Mass Transfer*, **120**, pp. 671-682 (2018).
26. Mukesh Kumar, P.C. and Arun Kumar, C.M., "Numerical evaluation of cooling performances of semiconductor using CuO/water nanofluids", *Heliyon*, **5(8)**, e02227 (2019).
27. Yang, L., Huang, J., Mao, M., et.al., "Numerical assessment of Ag-water nano-fluid flow in two new microchannel heatsinks: Thermal performance and thermodynamic considerations", *International Communications in Heat and Mass Transfer*, **110**, 104415 (2020).

28. Wiriyasart, S., Suksusron, P., Hommalee, C., et.al., "Heat transfer enhancement of thermoelectric cooling module with nanofluid and ferrofluid as base fluids", *Case Studies in Thermal Engineering*, **24**, 100877 (2021).
29. Zhao, N., Qi, C., Chen, T., et.al., "Experimental study on influences of cylindrical grooves on thermal efficiency, exergy efficiency and entropy generation of CPU cooled by nanofluids", *International Journal of Heat and Mass Transfer,* **135**, pp. 16-32 (2019).
30. Bakhtia, F.Z. and Si-Ameur, M., "A comparison of mixed convective heat transfer performance of nanofluids cooled heat sink with circular perforated pin fin", *Applied Thermal Engineering*, **159**, 113819 (2019).
31. Jahanbakhshi, A., Nadooshan, A.A. and Bayareh, M., "Cooling of a lithium-ion battery using microchannel heatsink with wavy microtubes in the presence of nanofluid", *Journal of Energy Storage,* **49**, 104128 (2022).
32. Al-Tae'y, K. A., Ali, E. H. and Jebur, M. N., "Experimental Investigation of Water Cooled Minichannel Heat Sink for Computer Processing Unit Cooling", *Journal of Engineering Research and Application*, **7(8)**, pp. 38-49 (2017).
33. Qi, C., Zhao, N., Cui, X., et.al., "Effects of half spherical bulges on heat transfer characteristics of CPU cooled by TiO2-water nanofluids", *International Journal of Heat and Mass Transfer*, **123**, pp. 320-330 (2018).
34. Gorzin, M., Ranjbar, A.A., and Hosseini, M.J., "Experimental and numerical investigation on thermal and hydraulic performance of novel serpentine minichannel heat sink for liquid CPU cooling", *Energy Reports*, **8**, pp. 3375-3385 (2022).
35. Karabulut, K., Buyruk, E. and Kılınç, F., "Grafen Oksit Nanoparçacıkları İçeren Nanoakışkanın Taşınım Isı Transferi ve Basınç Düşüşü Artışı Üzerindeki Etkisinin Düz Bir Boruda Deneysel Olarak Araştırılması", *Mühendis ve Makina,* **59(690)** , pp. 45-67 (2018).
36. Cengel, Y. and Cimbala, J. M., "*Fluid Mechanics: Fundamentals and Applications*", McGraw-Hill Education, New York, USA, 2006.
37. ANSYS Fluent Theory Guide, 2013.

Figure and table captions

Figures

Figure 1. a) Zalman ZM-WB3 Gold heat exchanger. b) A schematic representation of the heat sink [2]

Figure 2. Heat sink model a) Solid volume b) Fluid volume

Figure 3. Change of mean CPU temperature when using different fluids for different geometries

Figure 4. Change of maximum CPU temperature when using different fluids for different geometries

Figure 5. Contours of temperature distribution in use of different fluid in CPU; for left column a=5.5 mm, b=1.4mm and for right column a=5.5 mm, b=2 mm.

Figure 6. Variation of the thermal resistance of the nanofluids

Figure 7. Variation of the heat convection coefficients of the nanofluids

Figure 8. Variation of the Nusselt Number and Pressure Drop in case of using water in the heat sink

Tables

Table 1. Thermophysical properties of nanofluids and water at 304 K

Table 2. Velocity values and Reynolds numbers at constant flow (0.05 kg/s).

(a)

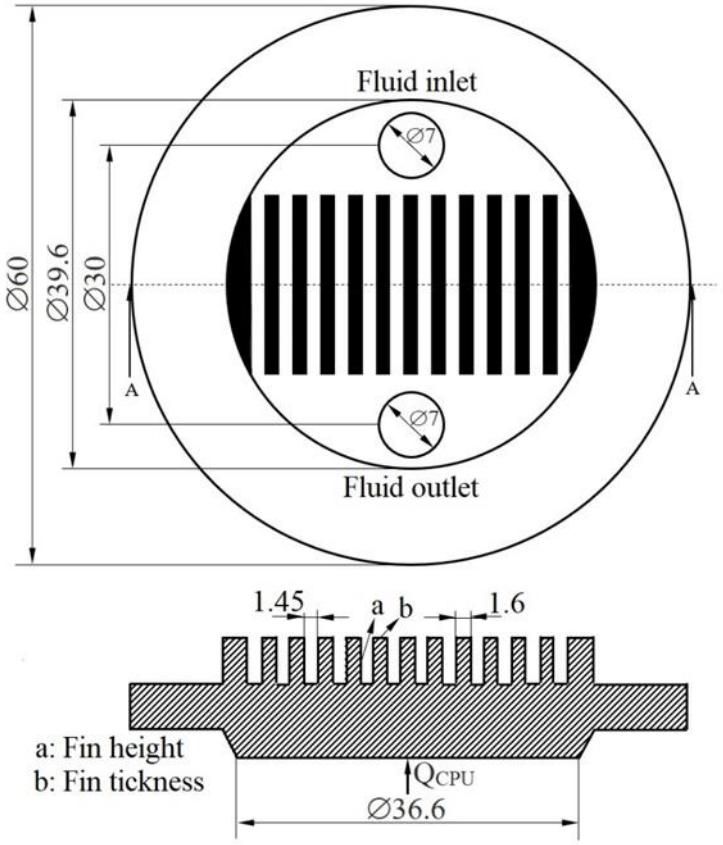

(b)

Figure 1. a) Zalman ZM-WB3 Gold heat exchanger. b) A schematic representation of the heat sink [2]

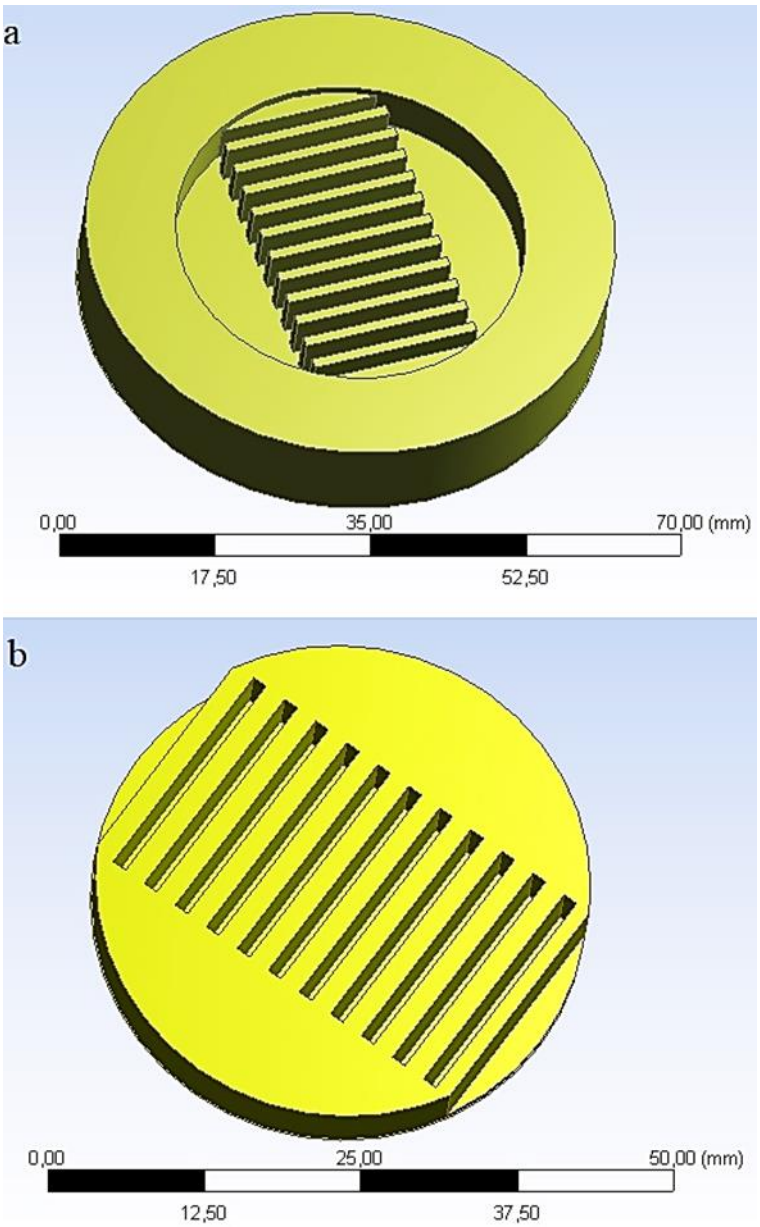

Figure 2. Heat sink model a) Solid volume. b) Fluid volume.

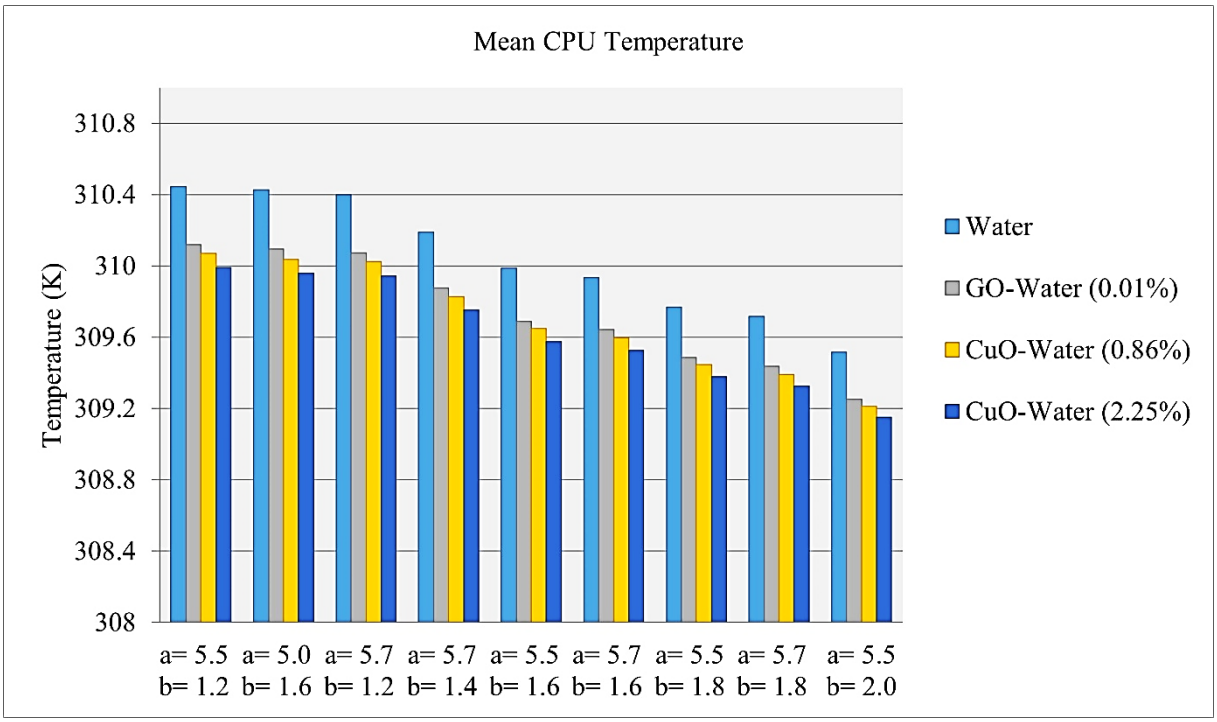

Figure 3. Change of mean CPU temperature when using different fluids for different geometries

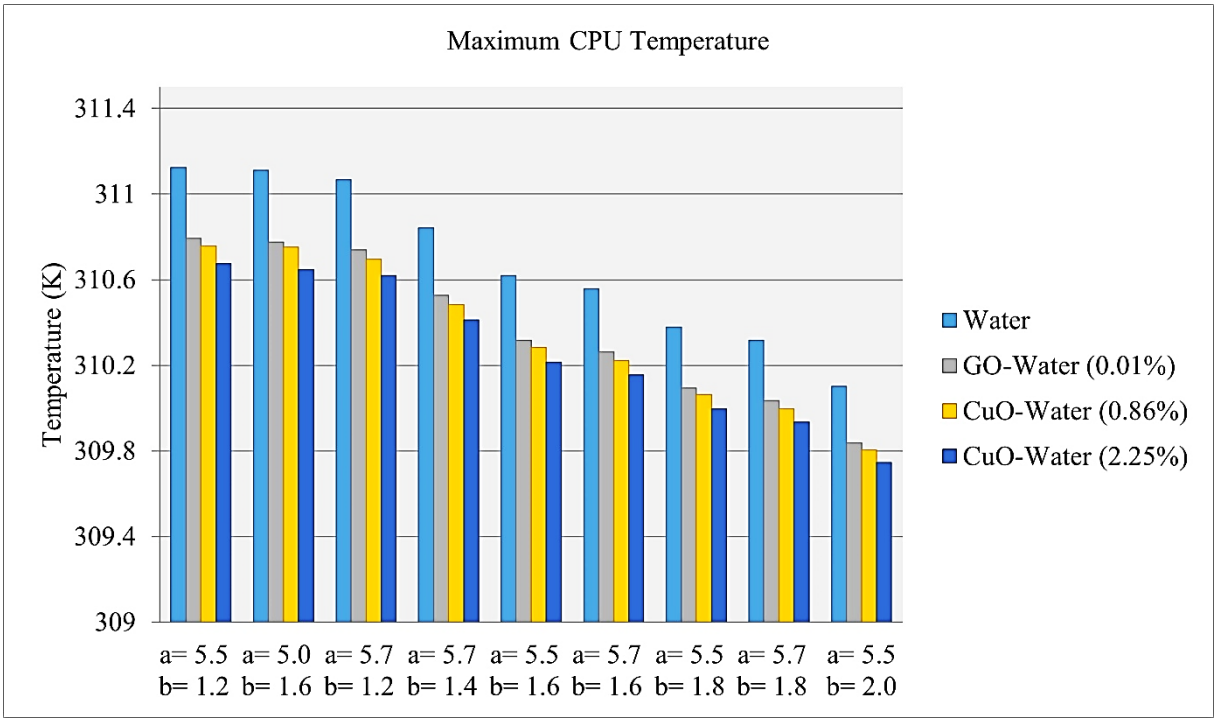

Figure 4. Change of maximum CPU temperature when using different fluids for different geometries

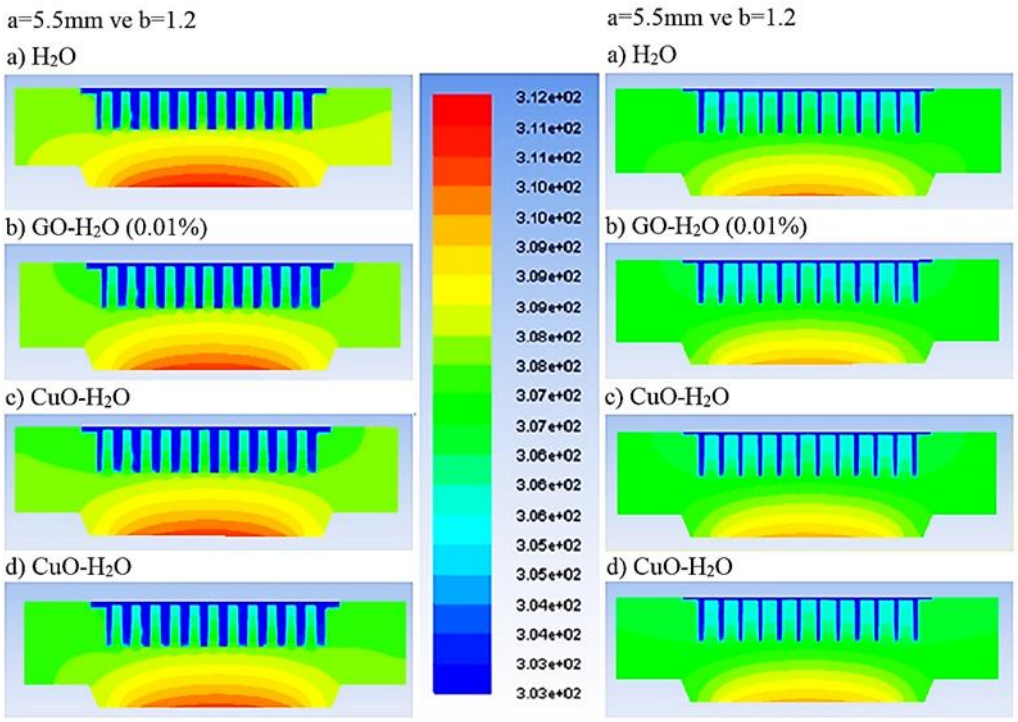

Figure 5. Contours of temperature distribution in use of different fluid in CPU; for left column a=5.5 mm, b=1.4mm and for right column a=5.5 mm, b=2 mm.

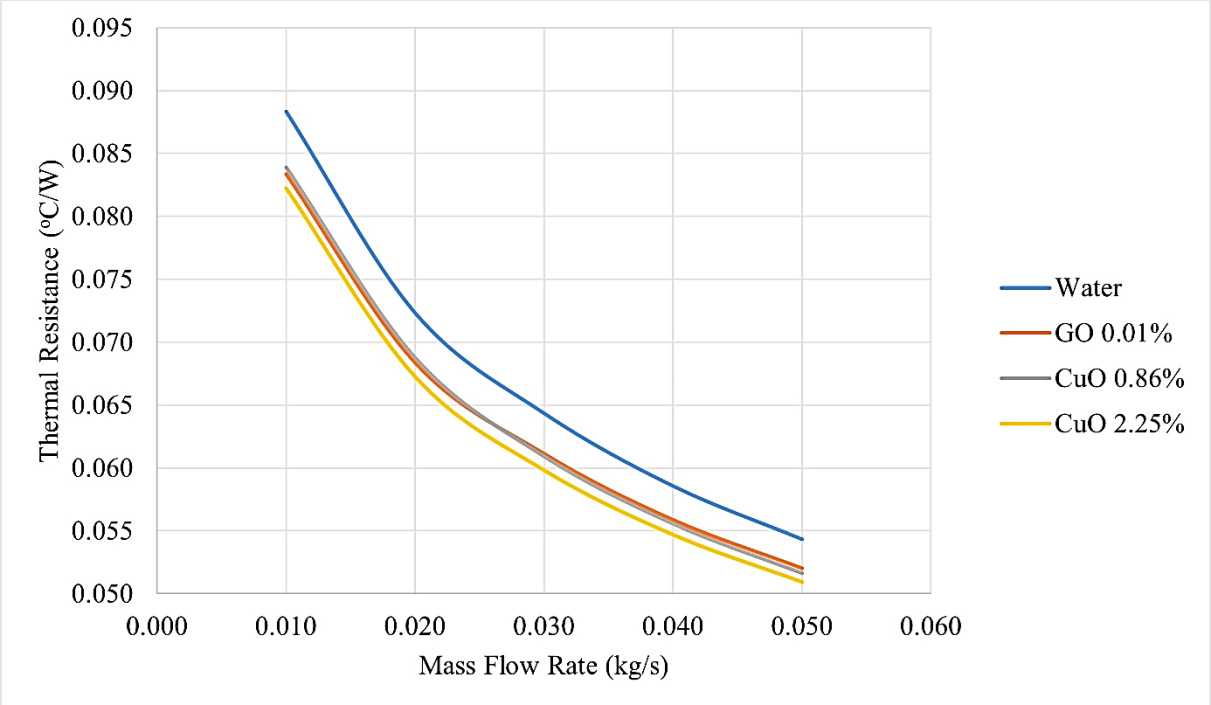

Figure 6. Variation of the thermal resistance of the nanofluids

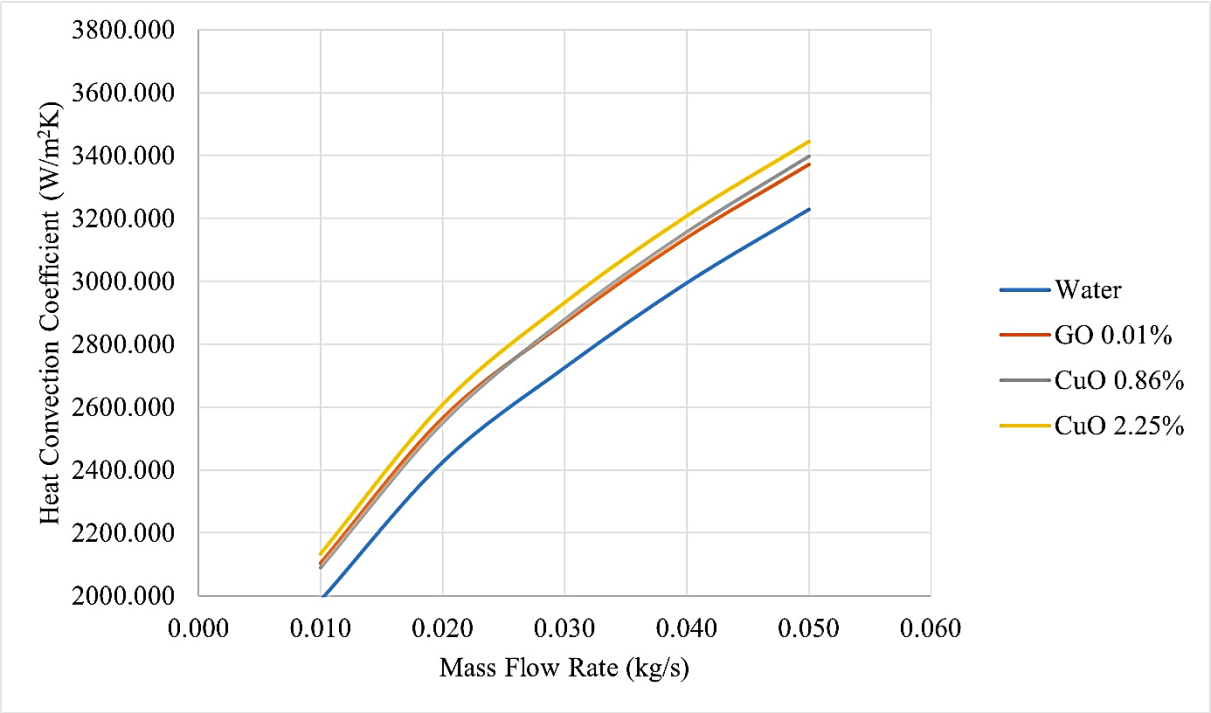

Figure 7. Variation of the heat convection coefficients of the nanofluids

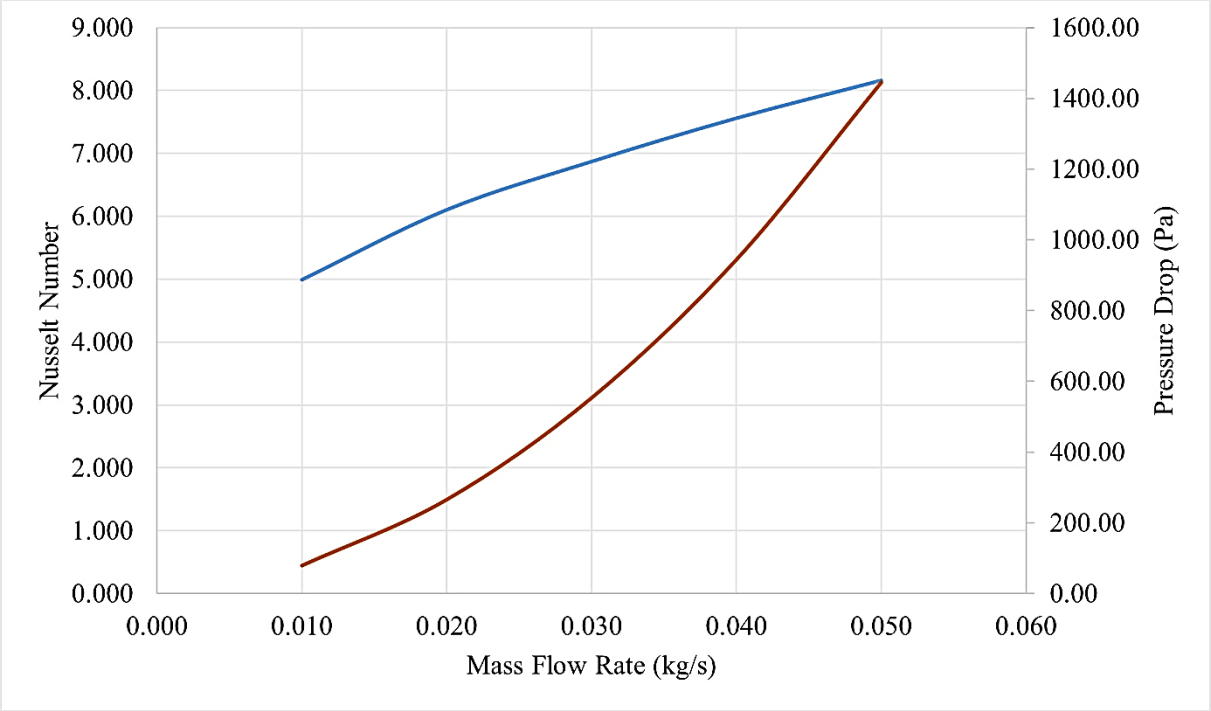

Figure 8. Variation of the Nusselt Number and Pressure Drop in case of using water in the heat sink

Tables

Table 1. Thermophysical properties of nanofluids and water at 304 K

	Base fluid	Nanoparticle	Volume fraction (%)	Thermal conductivity k (W/mK)	Specific heat Cp (J/kgK)	Dynamic viscosity μ (kg/ms)	Density ρ (kg/m^3)
1	water	-	0 (water)	0.6196	4178.4	0.000786115	994.86
2	water	CuO	0.86	0.6403	4078.21	0.000863488	1042.36
3	water	CuO	2.25	0.6848	3796.42	0.000870688	1117.69
4	water	GO	0.01	0.6696	4178.4	0.001	996.1

Table 2. Velocity values and Reynolds numbers at constant flow (0.05 kg/s).

		V (m/s)	Re
1	water	1.3059365	11 569.00
2	CuO (0.86%)	1.2464254	10 532.36
3	CuO (2.25%)	1.1624189	10 445.27
4	GO (0.01%)	1.3043108	9 094.568

Biographies

Gulnaz TOPCU: She received her B.Sc., M.Sc. degrees from Dumlupinar University Department of Mechanical Engineering. She is currently working as a design engineer in the machinery manufacturing industry. She deals with Computational Fluid Dynamics, Heat Transfer and Computer Aided Design and Manufacturing.

Umran ERCETIN: He received his B.Sc. in mechanical engineering from Dumlupinar University, M.Sc. and Ph.D. degrees in mechanical engineering from Eskisehir Osmangazi University. He is currently working as an Assistant Professor in Dumlupinar University Mechanical Engineering Department. He deals with Computational Fluid Dynamics, Heat Transfer, Refrigeraton, Heat Pumps, Drying and Energy Conversion Systems

Cisil TIMURALP: She received her B.Sc., M.Sc. and Ph.D. degrees from Eskisehir Osmangazi University Department of Mechanical Engineering. She is currently working as an Assistant Professor in Mechanical Engineering Department in the same university. She deals with Computational Fluid Dynamics and Heat Transfer.